



OPEN Thermal behavior and conversion of agriculture biomass residues by torrefaction and pyrolysis

Mihai Brebu✉, Daniela Ioniță & Elena Stoleru

Vegetal biomass is an abundant, readily available and easy to collect resource which can be converted into energy and materials. Biomass residues from agriculture and fruit crop activities, grouped in four classes (stalks, hulls, shells, pits), were subjected to thermal analysis and valorization. Thermogravimetry revealed high homogeneity between shells, large heterogeneity of stalks, and presence of thermally sensitive compounds in hulls. The Fisher weight variable selection analysis indicates that the differences in thermal behavior of biomass residues come from the components with specific biological functions (e.g. light volatiles and oils), while the structural components (hemicelluloses, cellulose and lignin) provide the general trend. This allows sample classification prior deciding on further waste management procedures. Torrefaction at 250 °C concentrated most part of the energy content into solids, with energy yield approaching 100%. Pyrolysis at 550 °C produces biochars with calorific values above 30 kJ/g from shells and pits. Most part of the energy input is used to produce oils with various compositions. Shells can be used to obtain phenolic compounds, hulls for production of aromatics and stalks for furans and ketones. Pits, on the other hand, are suitable raw material when fatty acids are targeted as pyrolysis compounds.

Keywords Thermal analysis, Torrefaction, Pyrolysis, Solid waste management, Product recovery

Biomass represents a ready available, accessible, important and versatile renewable resource which can be sustainably used for generation of alternative energy, chemicals and carbon based materials for daily basis use¹. Although biomass is very promising in replacing fossil-based sources, important challenges and difficulties are associated mainly in finding and developing of proper conversion and valorization methods². The main issue of biomass feedstock relies on the complex chemical structure and composition and on the highly oxygenated structure making it very reactive. This determines the necessity to develop new processes, reaction conditions, and catalytic materials suitable for biomass conversion to targeted applications and usage³.

Vegetal biomass from energy crops, forestry, orchards and agriculture residues or food industry waste can be a valuable source of energy^{4,5}. Besides being abundant resources, lignocellulosic residues are not competing with food chain in terms of land usage⁶. Vegetal biomass has different characteristics depending on species, part of the plant, and also on the geographical and climatic factors.

Besides basic characterization of biomass in terms of proximate, ultimate and compositional analysis, studies on thermal behavior are also of high importance. Thermogravimetry, which evaluates the thermal degradation of materials based on the mass loss or on the analysis of evolved volatiles (e.g. when coupled with FTIR or MS detection) can reveal the temperature range of degradation steps and the rates of associated processes, but also the differences among various samples⁷. These are valuable information especially when thermal methods such as hydrothermal treatments⁸, torrefaction⁹, pyrolysis¹⁰, gasification¹¹ and combustion¹² are preferred routes for the treatment and valorization of biomass and other polymeric solid waste. Thermal processing are among most preferred, being facile to operate at large scales and easily accommodating various types of raw materials^{13,14}.

Torrefaction, which is a thermal mild degradation at 200–300 °C in oxygen deficient atmosphere, gains strong interest in last decades, with several commercial plants being already operational¹⁵. This process stabilizes the biomass against natural decay by removing the moisture and the light volatiles¹⁶. It also breaks down the less thermally stable chemical bonds, mainly those from hemicelluloses but also from lignin, generating significant amounts of aqueous phase containing oxygen rich organic compounds¹⁷. This strongly decreases the oxygen content in the solid torrefied material, while increasing the carbon density. As a result, the torrefied biomass darkens towards blackish brown, become more hydrophobic and has increased porosity, compressibility and calorific value¹⁸.

"Petru Poni" Institute of Macromolecular Chemistry, 41 A Gr. Ghica Voda Alley, 700487 Iași, Romania. ✉email: bmihai@icmpp.ro

Pyrolysis uses high temperatures of 350–600 °C and inert atmosphere for advanced degradation that thermally breaks down the structural constituents of biomass into gases, aqueous fraction, oils and solid residue (biochar)¹⁹. Pyrolysis is one of the preferred methods for treatment and valorization of commingled waste, especially the hazardous ones²⁰. While hemicelluloses are among the less thermally stable structures in lignocellulosic materials, the labile chemical bonds in lignin starts to break down at temperatures as low as 170 °C, soon after removal of moisture²¹, lignin degradation continuing at slow rates over a broad range of temperature. The porosity generated by the evolution of volatiles from lignin has strong influence on cellulose degradation and on the reactivity of hemicelluloses²². The yield, quality and composition of pyrolysis products depend not only on processing parameters but mainly on the physical, chemical and structural properties of the biomass raw material²³. Especially the complexity of the pyrolysis oils requires proper selection of the input feed to facilitate good yield and composition of targeted products. Besides, process parameter can be used in data processing and machine learning to predict specific properties of the products^{24,25}.

We previously reported on thermal analysis and valorization of forestry residues^{18,26}. This is the second part of our work on biomass residues from agriculture and fruit crops activities. While the first part²⁷ explores the possibilities for discrimination and classification (including prediction) of biomass samples, as a preliminary step for decisions on proper waste management, the present paper focuses on using temperature as a facile and versatile tool both for analysis of biomass behavior and for converting biomass residue into value added products by torrefaction and pyrolysis.

Addressing the complex thermal behavior of biomass, which is one of the challenges for its valorization, with strong impact in controlling the valorization processes as well as the composition and the properties of the products, the originality of the work consists in (i) enhancing the power of basic TG analysis by statistical data processing and Fisher weight method to allow fast and clear identification of the factors differentiating the biomass samples, (ii) using integrative approach to correlate information from biomass characterization with composition and properties of thermal treatment products, (iii) comparatively analyzing biomass residues from various sources and parts of the plants to conclude on selecting the most suitable material and thermal procedure for targeted composition or properties of the obtained materials. Both papers in the study offer valuable information on characterization, selection and thermal conversion of agriculture and fruit crops biomass residue into valuable products for energy or chemicals, as a part of solid waste management.

Materials and methods

Materials

A number of 16 lignocellulosic residues from agriculture and fruit crops activities were considered for the study. Depending on the biological function, these were grouped in four classes: stalks (corn, sunflower, okra), hulls (walnuts, almonds, chestnuts, okra), shells (walnuts, almonds, hazelnuts, ginkgo) and pits (apricots, cherries, peaches, plums, okra). A very narrow area limited to a rural garden owned by one of the authors of the paper (hence permit for collection was granted) in the proximity of Iași city, Romania, (47°09'44"N, 27°35'20"E) was considered as a source of vegetal materials. This way the impact of geographical and pedoclimatic factors on the variability of biomass was minimized, at the expense of low number of species, which will be broadened in further studies.

After drying and size reduction, the biomass samples were characterized by proximate, ultimate and compositional analysis, as well as by FTIR spectroscopy and bomb calorimetry, which aided to discriminate among classes and to correctly predict the class of unknown samples. These results, presented in the first part of the study²⁷, are the starting and reference point for the work in this paper.

Methods

Thermogravimetry was performed on a Q5000 IR thermogravimetric (TG) analyzer (TA Instruments, USA). About 7 mg samples sieved below 0.1 mm were heated by 10 °C/min up to 900 °C in inert nitrogen flow of 25 mL/min.

Torrefaction and pyrolysis were performed at 250 and 550 °C, respectively, in a semi-batch process schematically presented before¹⁸. Briefly, about 10 g of biomass samples sieved below 5 mm were heated by 10 °C/min under self-generated atmosphere in a glass reactor (internal diameter of 25 mm, height of 320 mm). The liquid products, consisting mainly of an aqueous fraction in the case of torrefaction and of a mixture of aqueous and oily phases for pyrolysis, were collected in a graduate cylinder, while the solid residue was recovered from the bottom of the reactor at the end of the process. The non-condensable gaseous products were collected in a Teflon bag. The product yield was determined gravimetrically, with gas calculated by difference.

The calorific value (HHV) of the torrefied and pyrolysed biomasses was determined using an IKA C200 h bomb calorimeter (Staufen, Germany), using about 0.3 g powdered samples sieved below 0.5 mm. The energetic aspects of torrefaction and pyrolysis were evaluated based on the solid material. The energy density was calculated as the ratio between the calorific value of thermally processed (torrefied or pyrolysed) material and that of the raw, unprocessed biomass ($ED = \frac{HHV_{\text{processed}}}{HHV_{\text{raw}}}$). The energy yield was calculated multiplying the energy density by the solid yield ($EY = ED \times SY$).

The composition of the liquid products was determined by gas chromatography coupled with mass spectrometry (GC-MSD) using a 6890 N Agilent gas chromatograph which was coupled to a 5975 inert XL Agilent mass selective detector (Agilent, Santa Clara, CA, USA). A HP5-MS column with the length of 30 m, internal diameter of 0.25 mm and 0.25 µm thickness of (5%-phenyl)-methylpolysiloxane coated film was used under a temperature program of 40 °C(2 min) → 320 °C (10 °C/min) and helium flow of 1 mL/min. Injection was performed at 230 °C in 1:100 split mode and the GC to MSD transfer line was heated to 280 °C to avoid condensation of the products before reaching the detector. Qualitative identification was made based on NIST20 database with accepted quality of recognition above 85%. Confirmation of identified compounds was performed

based on calculated Kováts retention index^{28,29} which were compared with the ones from NIST20 database and on cross-checking among the 16 studied samples.

Results and discussion

Thermal analysis

The mass loss during thermal degradation of biomass usually occurs in several steps¹⁸, which overlap depending on sample composition – Fig. 1. Moisture is removed by evaporation below 100–110 °C. This is followed by the evaporation or degradation of light volatile compounds from the extractives, which can be seen as individual peaks or shoulders, usually below ~230 °C. Hulls are rich in volatile extractives, these acting as protective substances against the action of fungi or pests for the entire period of fruit formation and development before complete maturity. This explains the DTG peaks at 200–220 °C for all samples in Fig. 1.b, except for the okra pods, which have a different biological function. Pits also contain significant amounts of volatile compounds, being largely used for flavoring the alcoholic beverages³⁰. These are released as distinct DTG peaks or shoulders around 200–230 °C in Fig. 1.d. DTG shoulders around 165 °C and peaks at 220 °C could be also observed for the stalks of okra and corn (Fig. 1.a) while for the category of shells, only almonds present a small DTG peak at 143 °C and a shoulder around 241 °C (Fig. 1.c), also identified in the study of Debevc et al.³¹.

The thermal degradation of the structural components in biomass takes place in the 150–400 °C range³². The hemicelluloses are the least thermally stable and their fast decomposition appear as shoulders or broadening of the DTG peak below ~270 °C. Cellulose degrades in a narrower temperature range, with maximum rate around 350 °C. Lignin has a very complex structure; the most labile bonds break down with low rate at temperature as low as 170 °C while the main structure degrades slowly over a large temperature range. This is visible in Fig. 1.c, d as a long tail after the main peak of cellulose degradation, the shells and pits having by their nature higher lignin content.

The fourth step of mass loss in studied biomass residue occurs around 480–490 °C and is clearly visible only in very few samples, such as okra stalks and walnut hulls. The cross-linked structures remained after thermal degradation of lignin suffer advanced charring processes, with formation of light gases such as H₂, CH₄, CO and CO₂. Small mass loss and corresponding small DTG peaks could be observed around 650–680 °C for okra and sunflower stalks, as well as for walnut hulls and shells. Febrero et al.³³ showed that this stage is accompanied by the evolution of carbon dioxide, formed by decomposition of inorganic carbonates.

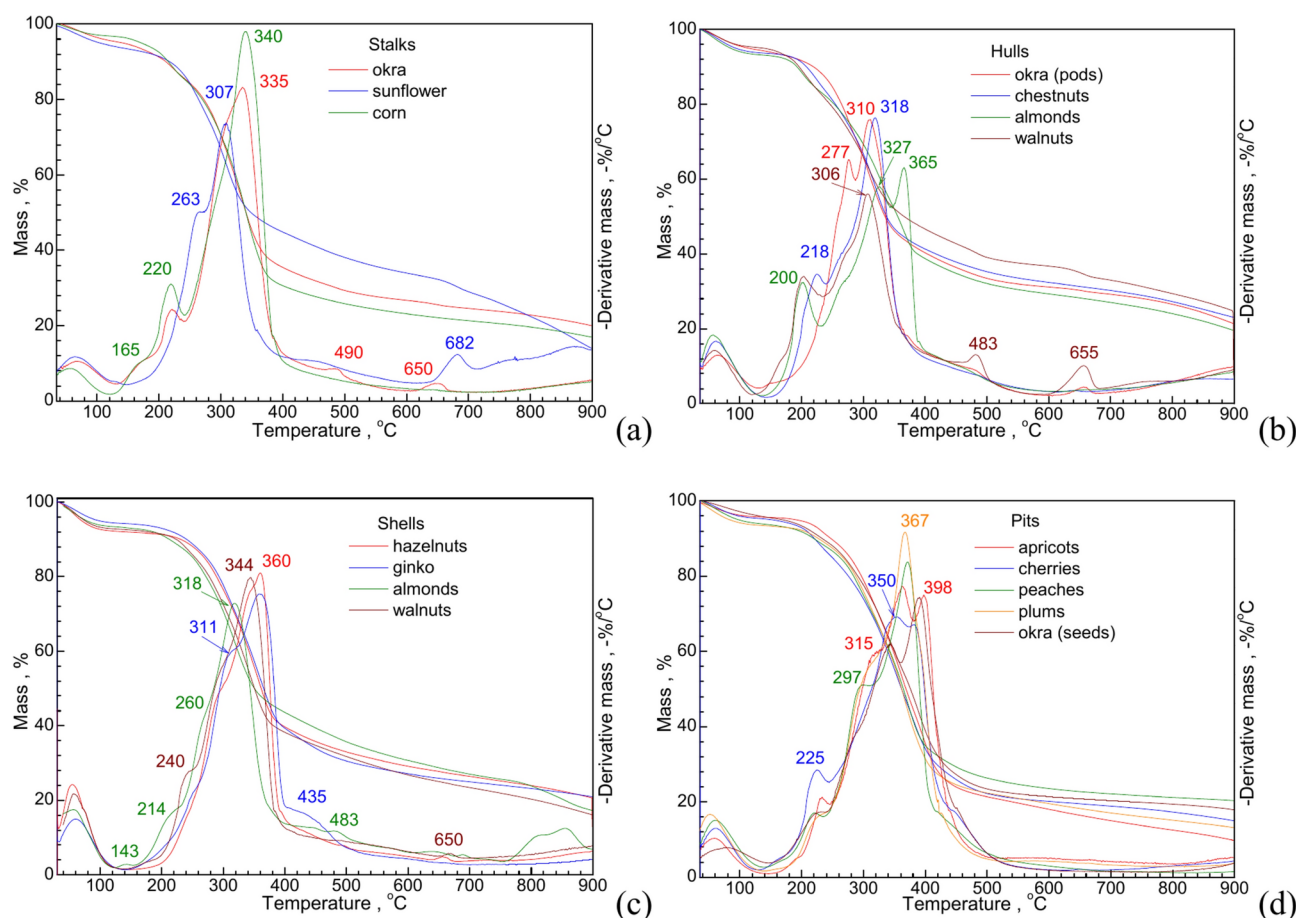


Fig. 1. TG/DTG curves of agriculture biomass residues from stalks (a), hulls (b), shells (c) and pits (d).

Besides some particularities of individual samples, similarities and differences among the four classes of agriculture biomass residues can be observed. The overlapped TG curves in Fig. 2a show that hulls have higher mass loss in the 180–280 °C temperature range, being rich in thermally sensitive compounds, most probably light extractives with biological active role, as previously discussed. However, they have the lowest total mass loss at 900 °C; this is due to the low total amounts of volatile matters, as presented in the first part of the study²⁷. Pits, on the contrary, have the highest mass loss, the TG curves at temperatures higher than 450 °C being below those of the other classes of samples. Shells have the highest homogeneity of samples within class, while stalks are largely heterogeneous, their TG curves being placed at high distance apart, especially at temperatures above ~380 °C, when thermal degradation of hemicelluloses and cellulose was ended. This can be explained by the most uniform composition in structural components (extractives, hemicelluloses, cellulose, lignin) of the shells, and by the large dispersion of fixed carbon and ash content in stalks, as discussed before²⁷.

Applying variable selection based on Fisher weight to the DTG data (processing in Matlab R2017b) allows identification of temperature ranges in which the differences between classes are statistically much higher than those within classes. The Fisher weight statistical method determines the weight of each variable (parameter that describes the samples in the system) as a measure of its ability to differentiate the groups of samples, by calculating the samples distances within groups compared with the distances between groups. Higher Fisher weight value of a variable indicates that the groups are better differentiating according to that variable. The deeper reds on the average DTG curve in Fig. 2b indicate larger variability of classes, while the deeper blues show higher similarities. Most significant differences in the thermal behavior are in the ~370–440 °C range, and especially between ~380 and ~396 °C, where the sigmoid shaped TG curves of stalks, hulls and shells already moved to the slowly declined part, while those of pits are still on the rapid descending range – Fig. 2.a. These occur at higher temperatures than the DTG peak around 350 °C for degradation of cellulose, and are in good agreement with the maximum mass loss of fatty acids reported by de Souza et al.³⁴ and Santos et al.³⁵. Significant differences, although smaller, can be also observed in the 198–208 °C temperature range corresponding to very light volatiles, presented especially in hulls. Interesting to note, the temperature ranges of ~275–287, 325–355 and 460–490 °C, corresponding to the degradation steps of the structural component in biomass, are those with the lowest Fisher weights. This is an indication that the differences between stalks, hulls, shells and pits as classes of agriculture biomass residues are generated mainly by the components with particular biological functions, such as fatty acids and light volatiles, and to very low extent by the main structural components (hemicelluloses, cellulose

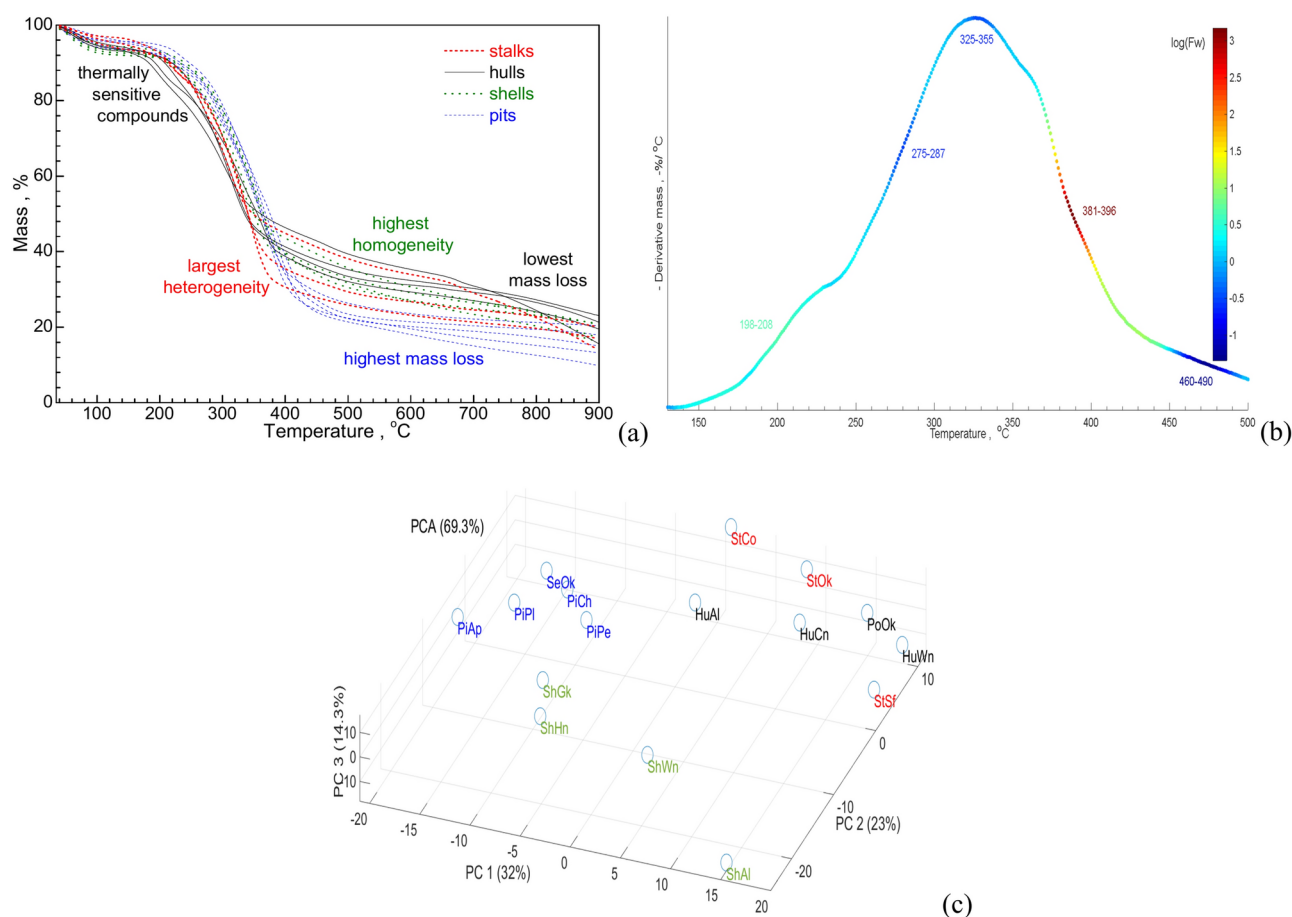


Fig. 2. Similarities and particularities in thermal behavior of agriculture biomass residues: overlapped TG curves (a), variable selection based on Fisher weight (b), and PCA (c).

and lignin), which give the general trend. Hence, thermogravimetry can be a valuable tool for identification of samples particularities with strong impact on thermal behavior and, consequently, on the thermal processing procedures and their products.

The above mentioned differences allow clear grouping of agricultural biomass residues when multivariate supervised methods such as principal component analysis (PCA) are used to differentiate samples with common features. Figure 2c shows that the first three principal components offer a very good description (~70%) of the entire set of DTG data in the range of 40–540 °C. Pits are discriminated from hulls and stalks by the first principal component, which have the major contribution of 32%, the particular thermal behavior being determined mainly by the oil components. Shells are separated by the other residues by the second principal component, which most probably describes the thermal behavior of lignin structural constituent. The stalk from sunflower is slightly apart from the stalks of corn and okra, the third principal component (PC3) contributing to this discrimination, especially due to lower mass loss above ~350 °C. Thermogravimetry appears to be also useful for sample classification before further processing for valorization.

Torrefaction

Figure 2b shows that the DTG shoulder corresponding to the very light volatiles ends around 250 °C. This temperature was selected to perform torrefaction, whose purpose is to remove the less stable thermally compounds. This is in good agreement with our previous observations on optimizing the torrefaction temperature for forestry residues²⁶.

Torrefaction removes between 20 and 40 wt% of the initial content of agriculture biomass waste, mainly as a liquid fraction (~15–28 wt%), only about 4–14 wt% being released as gases. Water is the highly dominant component of the liquid fraction; this results from the removal of moisture from the biomass samples (which is between 3.3 and 8.3 wt%) but also from the chemically bond water. Organic compounds are also formed by torrefaction, from the degradation of less thermally stable compounds such as extractives and hemicelluloses, but also from the breaking down of the most labile chemical bonds in lignin. These are mainly oxygenated compounds, with rather high polarity; these partition between the aqueous and the viscous, oily phase. The latter was in very small amounts and couldn't be successfully separated from the aqueous phase to determine its yield. Therefore, the liquid product was energetically mixed and the organic compounds were concentrated onto SPME fiber for GC-MSD analysis.

Differences in torrefaction yield can be observed between the agriculture biomass residues, both within but mainly between the classes in which these were grouped, according to their origin – Fig. 3a. Stalks produces the highest amount of gases and gives the lowest solid yield, while shells have opposite results, being also distinct by the lowest liquid yield. The latter can be explained by the highest lignin and lowest extractive content of shells²⁷.

The product yields from hulls and pits are not statistically different; however, pits have slightly larger dispersion and the average and median values are smaller for the solid residue and higher for the liquid product compared with hulls – Supplementary Fig. 1a. Some dispersion within classes can be observed in the solid and liquid yield, but these compensate, the gas yield being rather uniform.

The calorific value of the torrefied biomass is above 20 kJ/g, higher than of the initial agriculture residues, with about 20–40% for stalks, hulls and shells. This leads to energy density (calorific value of torrefied material versus that of initial, unprocessed biomass) of 1.2–1.4 after the thermal process – Fig. 3b. Pits show the lowest energy density, which is below 1.2. Considering that pits have low amounts of ash, and that oxygen is the main factor which decreases the calorific value, it appears that oxygen in pits is present in compounds with rather high thermal stability, which could not be totally removed by torrefaction at 250 °C. Consequently, the energy yield (energy density multiplied by solid yield) of torrefaction, calculated based on the solid residue, is only below 80% for pits, smaller than for stalks, hulls and shells. Energy yields reach values close to 100% for shells, making torrefaction an energetically favorable treatment process for this class of agriculture biomass residues. This is because the calorific energy is better stored in lignin, which has lower oxygen content (~30%) compared

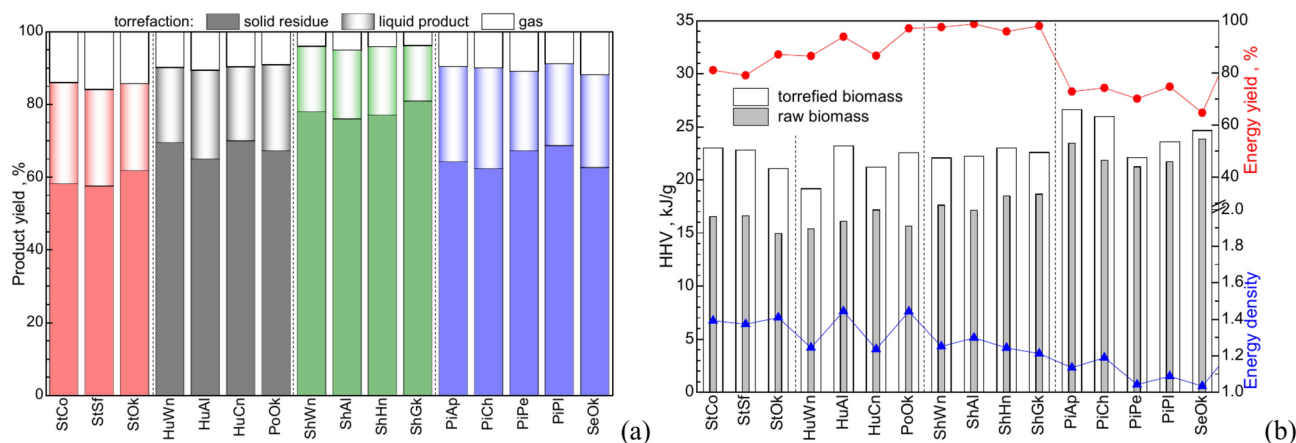


Fig. 3. Torrefaction of agriculture biomass residue: product yield (a) and energetic values of the solid residue (b).

with ~50% for cellulose, and can compensate the energy spent in the thermal process to decrease the oxygen content by removing the moisture, part of the chemically bonded water and of light volatiles.

The composition of organic compounds in the liquid fraction is described in Fig. 4 by the aid of the NP-gram curves. These graphically represent the amount of compounds (expressed as GC-MSD area percent) versus the carbon number, which is the integer down rounded Kováts retention index divided by 100 (e.g. a Kováts index of 1056 corresponds to nC10), and is equivalent to the boiling point range of normal paraffins. The NP-grams, proposed by Murata and Makino³⁶, are useful for rapid visualization of the differences in the global composition of various liquid samples and can substitute, with the benefit of very small sample amount (order of microliters) and faster analysis time, the distillation curves largely used in petrochemical chemistry.

Torrefaction produces high amounts of acetic acid (the main peak at nC6 in the NP-grams). This is a degradation product of hemicelluloses, but is also released from the pyrolysis of lignin, the latter being acetylated in herbaceous biomass³⁷. Besides acetic acid, furans (e.g. furfural, furanmethanol, dihydrobenzofuran, hydroxymethylfurfural) are the main products of torrefaction. They appear in the nC8–nC12 range of the NP grams and are results of hemicelluloses degradation. Presence of cresols and guaiacol at nC10 and of syringol at nC13 confirms that thermal degradation of labile bonds in lignin is also initiated during torrefaction at 250 °C.

Clear differences can be observed in the composition of organic compounds of agriculture biomass residues, both between and within classes. Shells have limited amounts of compounds in the nC11–nC18 range and no compound heavier than nC18 – Fig. 4c. Interesting to note is the distinction of ginkgo among other shells, with high amounts of furfural and lower contribution of acetic acid. Stalks have rather equilibrate distribution of furans in the nC8–nC14 range, while these are narrowed to nC8–nC10 range in hulls – Fig. 4a, b. However, the stalks of sunflower, which are richer in lignin, show cresols and guaiacol as main compounds at nC10, while the stalks of okra, having less hemicelluloses, gave lower amounts of dihydrobenzofuran at nC12. The okra pods have the lowest lignin content in the class in which they were included (hulls) but they produce syringol as the main torrefaction compound at nC13. This is an indication that the lignin in okra pods is of syringyl type, thus less thermally stable. Pits show high peaks at nC19 and nC21, these being the dominant ones in the composition of okra seeds – Fig. 4d. These peaks stand for fatty acids (e.g. palmitic, linoleic, vaccenic), which are part of the oil composition of pits. Since their thermal stability range is above 250 °C, it is expected that most part of acids remain in the torrefied pits, confirming the discussion above regarding the calorific values and energy density.

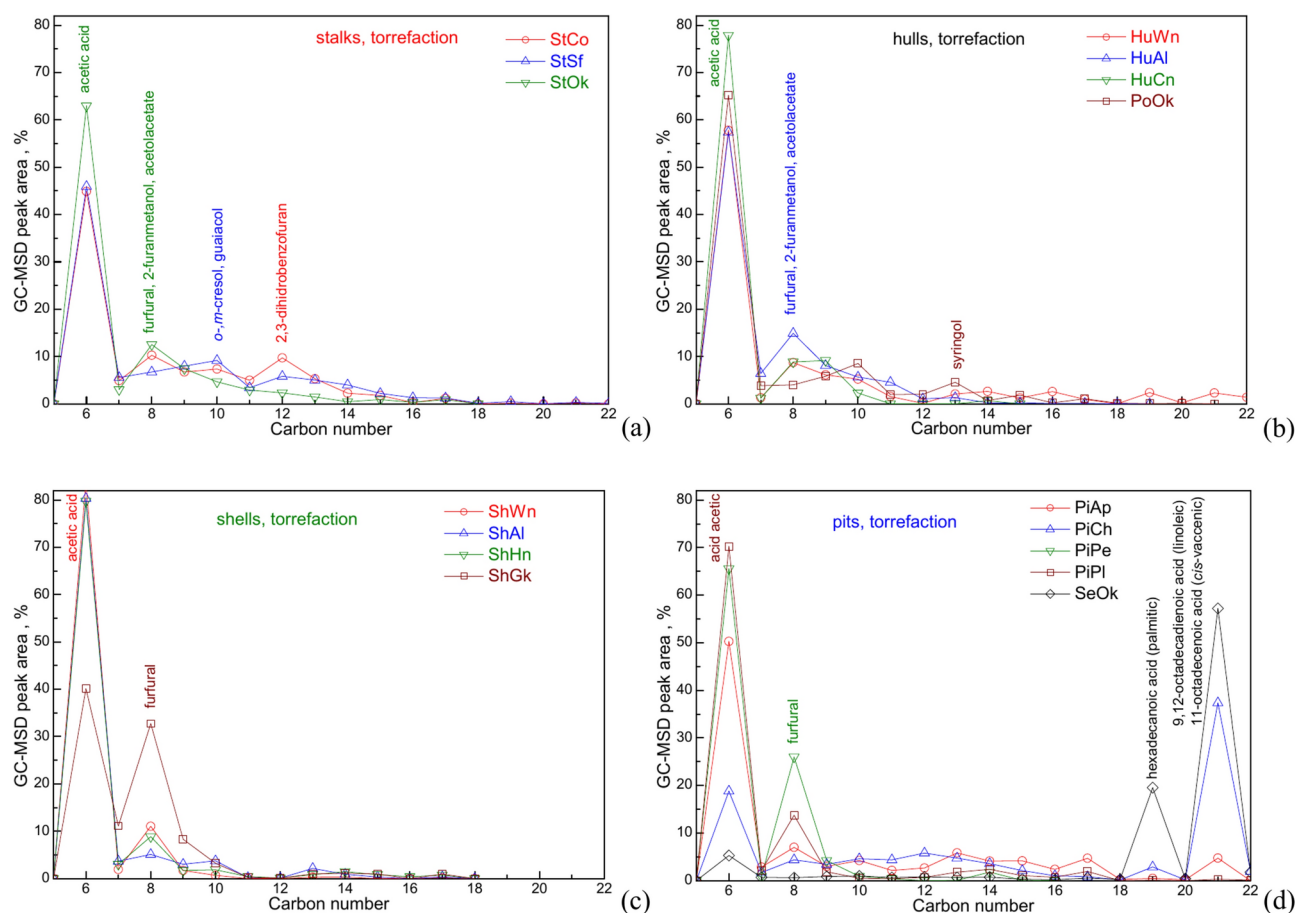


Fig. 4. The NP-grams of the organic compound in liquid fractions from the torrefaction of stalks (a), hulls (b), shells (c) and pits (d).

Okra seeds are the richest ones in fatty acids, these being also present in stalks, although in lower amounts, thus less visible in the NP grams in Fig. 4a.

Pyrolysis

The TG/DTG data in Fig. 1 shows that thermal degradation of agriculture biomass residues ends before about 550 °C. Hence, this temperature was selected for pyrolysis experiments, in good agreement with our previous observations on optimum pyrolysis temperature for forestry residues²⁶.

Pyrolysis, being a thermal process of advanced degradation, strongly decreased to 20–25 wt% the amount of solid residue remaining from stalks, shells and pits – Fig. 5a. Hulls show higher solid yields of 26–31 wt%, in good agreement with the lowest mass loss observed from the TG curves in Fig. 2a. Most part of organic compounds produced from the pyrolysis of biomass remain in the form of dark brown, viscous and sticky oil fraction, which accounts for 30–38 wt% of the product yield. The aqueous phase represents 3–14 wt% of the initial material and has yellow-reddish colour and a turbid aspect. This is due to the more polar pyrolysis compounds which partition between the oil and aqueous phase and help stabilizing the emulsion if the two phases are energetically mixed. Especially the phenol derivatives were found to act as efficient surfactants which are able to keep apart drops of melted plastics in aqueous media³⁸. Although stalks produce slightly higher oil yields, pits give more aqueous phase – Supplementary Fig. 1b, leading to the highest liquid (oil + aqueous phase) yield (more than 44.5 wt%), in good agreement with the highest mass loss above 450 °C observed by thermogravimetry – Fig. 2a.

The advanced degradation of biomass strongly increases the formation of gases, with yield of 30–36 wt% reaching that of the oil product – Supplementary Fig. 1b. However, it is to be mentioned that the pyrolysis of lignin leads to high amounts of compounds with high heat capacity, such as guaiacol and syringol, with $C_{p,gas}$ of 205 and 268 J/mol.K at 216 and 266 °C, respectively^{39,40}. These are difficult to cool down and condensate as liquid product and, most of the time, can partly escape in gaseous products, artificially increasing the yield. Within classes, pits provide less disperse aqueous and gas yields, while shells give more uniform solid yield – Supplementary Fig. 1b; this could be due to closer amounts of structural components determined by compositional analysis²⁷.

Pyrolysis removes most part of oxygen in biomass as pyrolytic water and oil, increasing the carbon content of the solid residue. This improves the calorific values, which exceed 25 kJ/g for stalks and hulls and 30 kJ/g for shells and pits – Fig. 5b. Consequently, the energy density is in the range of 1.4–1.8, much higher than for torrefaction. Since the solid yield is strongly diminished, the energy yield is in the range of 32–48%. This is because high energy input is needed for advanced breakdown of cellulose and lignin structure, most part of initial energy content of biomass being transferred to pyrolysis oils.

Most part of the compounds in the pyrolysis oils of the biomass residues from agriculture and fruit crops activities are distributed in the nC8–nC14 range of carbon numbers. Stalks, which are rich in cellulose but have various contents of hemicelluloses show distinct peaks of furans and ketones, at nC8, nC10 and nC12, corresponding mainly to furfural, furfuryl alcohol and acetol acetate at nC8 for okra, to cresols and guaiacol for sunflower and to furans for corn – Fig. 6a. This pattern is similar with that of torrefaction, being dependent on the composition and structure of stalks.

Hulls, shells and pits have more lignin and less cellulose (especially for shells) compared with stalks. Therefore, the nC9–nC13 range of the NP grams in Fig. 6b–d is dominated by phenol and its methoxy derivatives, furans being dominant at nC8. Heavier compounds such as methylsyringol and eugenol at nC14, trimethoxytoluene at nC15 and propenylsyringol at nC17 are produced in higher amounts from shells (walnuts and almonds) and pits (plums). The fatty acids at nC19 (palmitic acid) and nC21 (linoleic and vaccenic acid) are observed in small amounts from the pyrolysis of shells but are significant in stalks, hulls and especially in pits. Particularly, pyrolysis of okra seeds gave mainly fatty acids (~77 GC-MSD area percent), the other compounds, in the nC8–nC14 range, representing only ~5.3% of the total chromatographic area.

Pyrolysis, being a highly energetic degradation method, converts biomass into a wide range of chemical compounds from various classes⁴¹, the chromatograms being complex, usually revealing more than 100

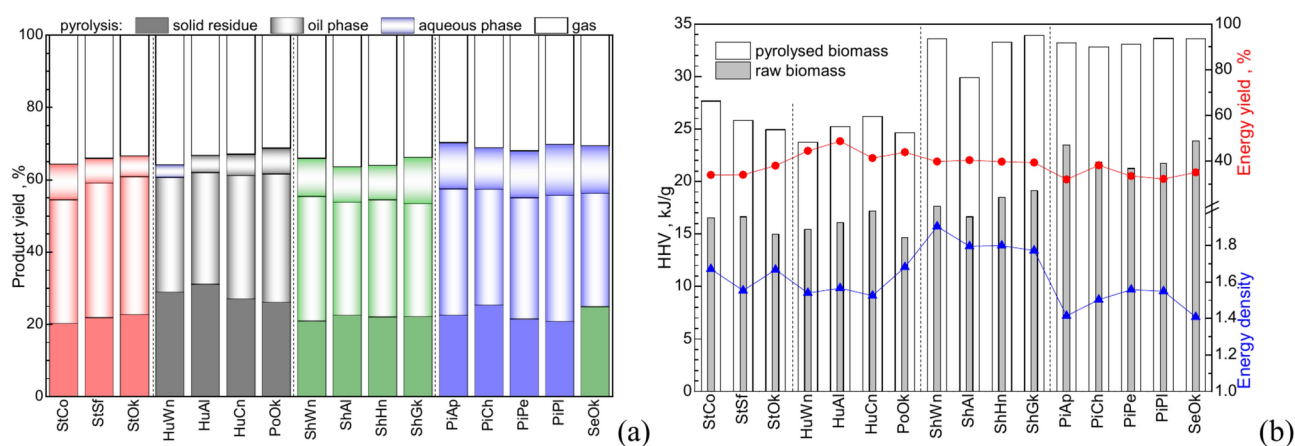


Fig. 5. Pyrolysis of agriculture biomass residue: product yield (a) and energetic values of the solid residue (b).

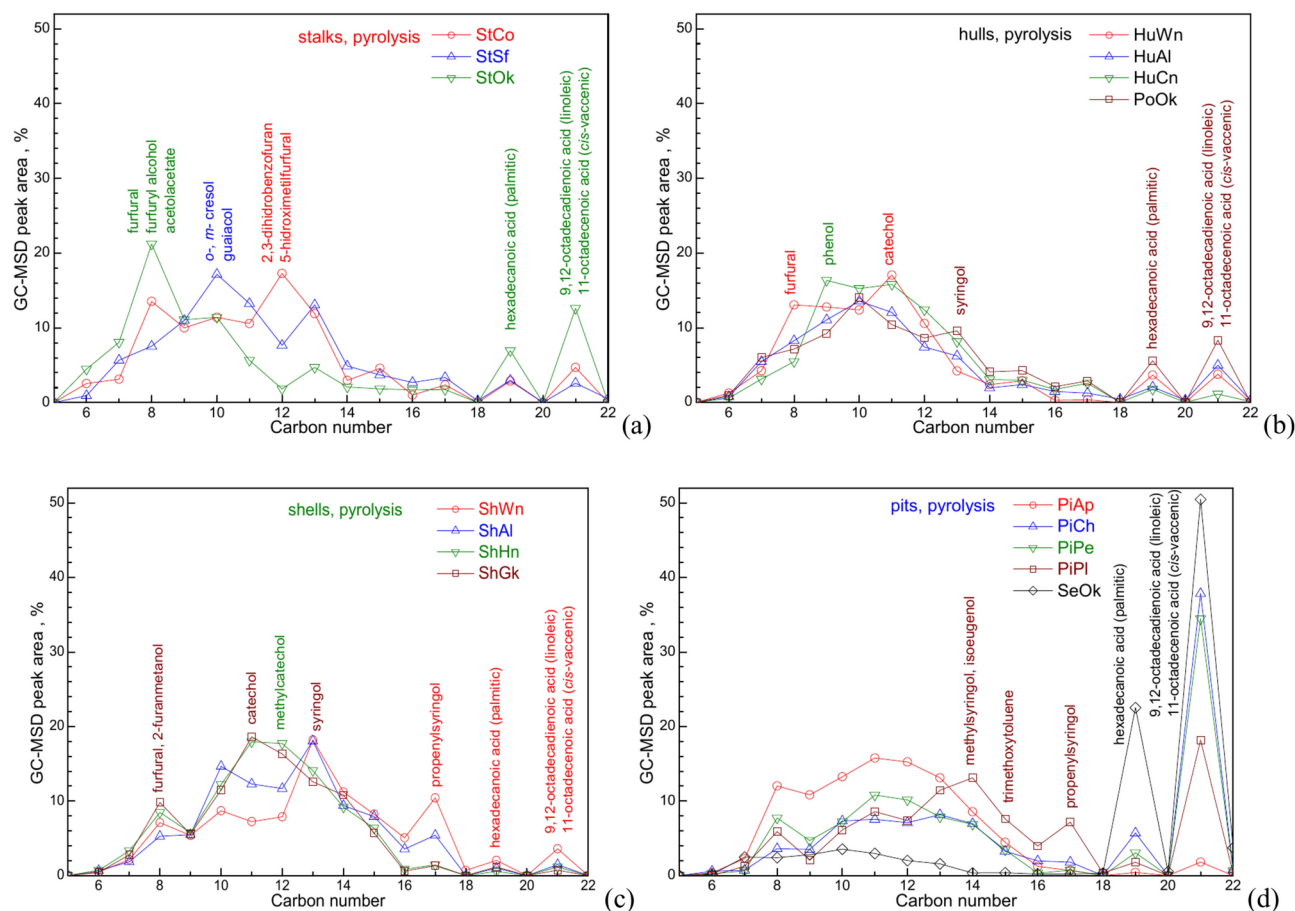


Fig. 6. The NP-grams of the organic compound in liquid fraction from pyrolysis of stalks (a), hulls (b), shells (c) and pits (d).

compounds. While most of these are in very small amounts, below 1%, they can impact the properties of pyrolysis oils in a similar manner in which the numerous small compounds synergistically contribute to the bioactivity of the major components in essential oils⁴².

The pyrolysis compounds produced in significant amounts (chromatographic peak area higher than 1%) according to their chemical class are listed in Table 1.

Acetic acid, furfural and its derivatives, ketones, and small amounts of aldehydes and alcohols are mainly originating from hemicelluloses⁴³. Furans and light oxygenated compounds are also produced from thermal degradation of cellulose⁴⁴. Lignin, on the other side, produces phenolic derivatives, but also aromatics.

Formation of different classes of compounds from pyrolysis of agriculture biomass residues is summarized in Fig. 7. Besides the total amount of compounds formed from each sample, the heatmap also presents in blue scale the relative yield for each class of compounds obtained from different sources. The main chemicals in the pyrolysis oils are the *phenolic* derivatives, especially the methoxylated ones, resulted from the thermal degradation of lignin. These are produced especially from the pyrolysis of shells (53–61%), which are the richest one in lignin, and to the lowest extent from stalks. Deoxygenated *aromatic* compounds are also formed, especially from hulls, their amount (7–12%) being significantly higher than for the other biomass samples. Okra pods produced the highest content of *ketones* (8.5%). While okra pods were included in the class of hulls based on the biological role of protecting the fruits/seeds, they are closer in composition to stalks, whose pyrolysis generate 5–7% ketones, compared with maximum 2.3% produced by hulls (except for the okra pods), shells and pits (with negligible yield of ketones). *Furans* are also produced in highest amounts by stalks, reaching 22% in the case of corn. Both furans and ketones are highly oxygenated compounds resulted from thermal degradation of the saccharide content in biomass. *Acids* consist of acetic acid, produced from thermal degradation of structural components in biomass, and of fatty acids, which can be present in biomass to play specific biological role. Pits are rich in fatty acids, as energy reserve for seeds sprouting. Therefore pits are the biomass residues which produce the highest amounts of fatty acids, around 40–45% for cherries and peaches, and up to 67% for okra seeds. The stalks and the pods of okra also produce the highest amounts of fatty acids among the other samples in their classes (stalks and hulls). These data and their interpretation are valuable in deciding the biological source for obtaining specific types of chemicals by pyrolysis as a thermal valorization method.

No	Retention time	Carbon number	Class	Name	CAS number
1	2.15	nC5	Ketones	2-Butanone	78-93-3
2	2.49	nC6	Acids	Acetic acid	64-19-7
3	2.69	nC6	Aromatics	Benzene	71-43-2
4	2.73	nC6	Ketones	Acetol	116-09-6
5	4.15	nC7	Aromatics	Toluene	108-88-3
6	5.30	nC8	Furans	Furfural	98-01-1
7	5.67	nC8	Furans	Furfuryl alcohol	98-00-0
8	5.82	nC8	Aromatics	Ethylbenzene	100-41-4
9	5.89	nC8	Ketones	Acetol acetate	592-20-1
10	5.98	nC8	Aromatics	Xylene (1,3)	108-38-3
11	6.39	nC8	Aromatics	Xylene (1,2)	95-47-6
12	6.61	nC9	Ketones	2-Methyl-2-cyclopentenone	1120-73-6
13	6.67	nC8	Furans	Acetylfuran	1192-62-7
14	7.62	nC9	Furans	5-Methylfurfural	620-02-0
15	7.64	nC9	Aromatics	Ethylmethylbenzene	620-02-0
16	7.66	nC9	Ketones	3-Methyl-2-cyclopentenone	2758-18-1
17	7.90	nC9	Phenols	Phenol	108-95-2
18	8.71	nC10	Aromatics	Trimethylbenzene	95-63-6
19	8.74	nC10	Ketones	3-Methyl-1,2-cyclopentanedione	765-70-8
20	8.93	nC10	Ketones	2,3-Dimethyl-2-cyclopentenone	1121-05-7
21	9.23	nC10	Phenols	<i>o</i> -Cresol	95-48-7
22	9.52	nC10	Phenols	<i>p</i> -Cresol	106-44-5
23	9.77	nC10	Phenols	Guaiacol	90-05-1
24	10.14	nC11	Phenols	2,3-Dimethylphenol	526-75-0
25	10.25	nC11	Ketones	3-Ethyl-2-hydroxy-2-cyclopenten-1-one	21,835-01-8
26	10.97	nC11	Phenols	Ethylphenol	620-17-7
27	11.39	nC11	Phenols	Catechol	120-80-9
28	11.78	nC12	Furans	Dihydrobenzofuran	496-16-2
29	11.92	nC12	Furans	Hydroxymethylfurfural	67-47-0
30	12.08	nC12	Phenols	4-Isopropylphenol	99-89-8
31	12.38	nC12	Phenols	Homocatechol	452-86-8
32	12.67	nC12	Phenols	<i>p</i> -Ethylguaiacol	2785-89-9
33	12.86	nC12	Phenols	4-Methylcatechol	452-86-8
34	13.18	nC13	Phenols	<i>p</i> -Vinylguaiacol	7786-61-0
35	13.66	nC13	Phenols	3,4-Dimethoxyphenol	2033-89-8
36	13.69	nC13	Phenols	Syringol	91-10-1
37	14.12	nC13	Phenols	4-Ethylcatechol	1124-39-6
38	15.05	nC14	Phenols	Isoeugenol	97-54-1
39	16.03	nC15	Phenols	Guaiacylacetone	2503-46-0
40	16.42	nC15	Phenols	4-Vinylsyringol	28,343-22-8
41	17.99	nC17	Phenols	Propenylsyringol	20,675-95-0
42	21.70	nC19	Acids	Palmitic acid	57-10-3
43	23.33	nC21	Acids	Linoleic acid	60-33-3
44	23.40	nC21	Acids	Oleic acid	506-17-2
45	23.63	nC21	Acids	Stearic acid	57-11-4

Table 1. The main identified compounds in the pyrolysis oils of agriculture biomass residues.

Conclusions

The effect of temperature in terms of thermal analysis to determine the degradation behavior and of thermal treatment/valorization procedure to generate valuable products was studied on several agriculture biomass residues. These were grouped in four classes (stalks, hulls, shells and pits) according to the biological function.

Although following a general pattern, the thermal behavior strongly depends on sample characteristic, determined by the proximate and especially by the compositional analysis. Particularities within classes, such as large heterogeneity for stalks and high homogeneity of shells and between classes (lowest and highest mass loss for hulls and pits, respectively, and presence of thermally sensitive compounds in hulls) could be observed. Using Fisher weight statistical evaluation on thermogravimetry data concluded that the differences between stalks,

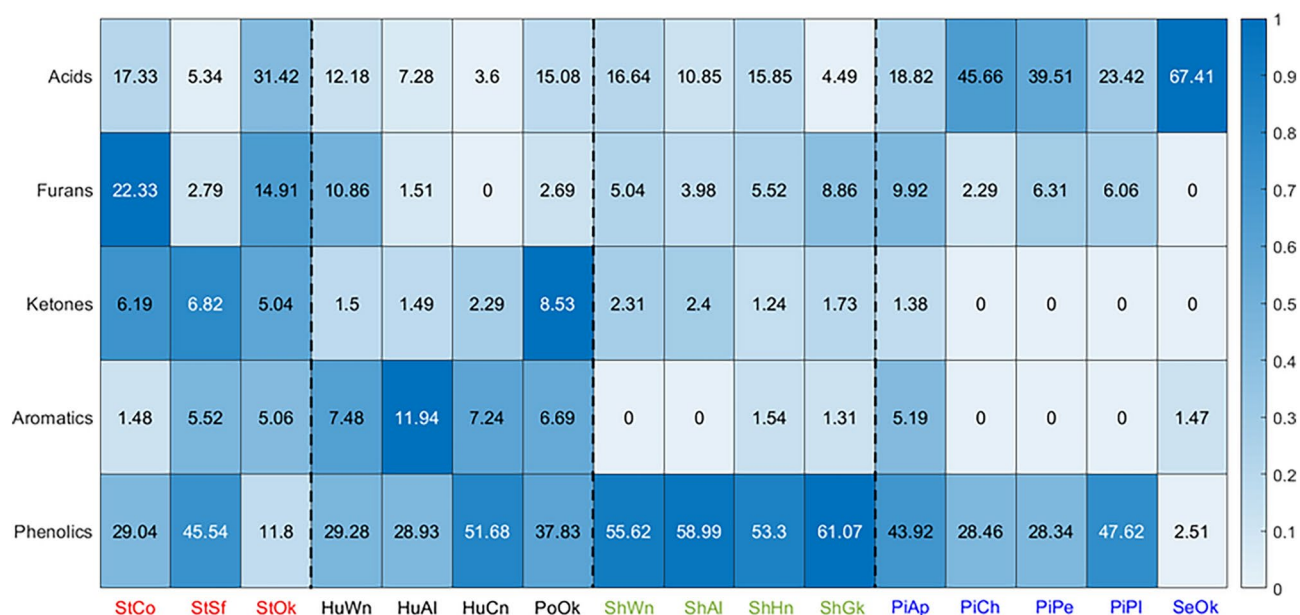


Fig. 7. The heatmap of the main classes of compounds produced from the pyrolysis of agriculture biomass residues.

hulls, shells and pits are coming from the components with particular biological functions, such as light volatiles and oils, and not from the main structural components (hemicelluloses, cellulose, lignin), which give the general trend. Grouping of biomass samples according to thermal behavior was possible by PCA, potentially serving as a classification method prior deciding on best treatment/valorization procedure.

Torrefaction at 250 °C and pyrolysis at 550 °C, performed in a semi-batch reactor, were discussed for the energy content of the solid residue and for the chemical composition of the liquid products. Torrefaction produces high amounts of acetic acids and furans, mainly from the degradation of hemicelluloses in biomass residues, but also of fatty acids from the extractive compounds in pits. It is also a highly energy efficient process, its energy yield approaching 100% for the treatment of shells.

Pyrolysis enhances with 40–80% the high heating values of the solid residues, which can be used as superior fuels, especially for shells and pits. However, these are obtained in small amounts of only 20–30 wt%, most part of the energy content in biomass being transferred to the pyrolysis oils. Pyrolysis also generates acids, furans, ketones, aromatics and phenols as the main classes of compounds from the degradation of carbohydrate and of lignin structure in biomass. The amounts strongly depend on the biomass source. Shells can be used for production of phenolics, hulls for generation of aromatics while stalks provide highest amounts of ketones and furans. Pits and especially okra seeds are to be used when recovery of fatty acids is targeted.

The results of torrefaction and pyrolysis experiments confirm that the particularities and classification of biomass residues from agriculture and fruit crops activity, revealed by thermogravimetry, strongly affect the properties of the products after thermal treatment. Moreover, the thermal behavior information can be used in selection of the thermal treatment method and of the biomass class when special requirements related with the energy efficiency of the process or the quality and composition of the products.

Data availability

Data will be available on request from the corresponding author.

Received: 30 September 2024; Accepted: 23 January 2025

Published online: 03 April 2025

References

- Nunes, L. J. R., Casau, M., Dias, M. F., Matias, J. C. O. & Teixeira, L. C. Agroforest woody residual biomass-to-energy supply chain analysis: Feasible and sustainable renewable resource exploitation for an alternative to fossil fuels. *Results Eng.* **17**, 101010. <https://doi.org/10.1016/j.rineng.2023.101010> (2023).
- Nzihou, A. Toward the valorization of waste and biomass. *Waste Biomass Valor.* **1**, 3–7. <https://doi.org/10.1007/s12649-010-9014-x> (2010).
- Serrano-Ruiz, J. C. Biomass: A renewable source of fuels, chemicals and carbon materials. *Molecules* **25**, 5217. <https://doi.org/10.3390/molecules25215217> (2020).
- Global biomass potential towards 2035, World Bioenergy Association, Stockholm, Sweden, 2015. http://www.worldbioenergy.org/uploads/Factsheet_Biomass%20potential.pdf. Accessed 2 Sep 2024. (2024).
- Scarlat, N., Dallemand, J.-F., Monforti-Ferrario, F., Banja, M. & Motola, V. Renewable energy policy framework and bioenergy contribution in the European Union—An overview from national renewable energy action plans and progress reports. *Renew. Sustain. Energy Rev.* **51**, 969–985. <https://doi.org/10.1016/j.rser.2015.06.062> (2015).

6. Kabir, G. & Hameed, B. H. Recent progress on catalytic pyrolysis of lignocellulosic biomass to high-grade bio-oil and bio-chemicals. *Renew. Sustain. Energy Rev.* **70**, 945–967. <https://doi.org/10.1016/j.rser.2016.12.001> (2017).
7. Bedoui, A., Souissi-Najar, S., Idris, S. S., Abd Rahman, N. & Ouederni, A. Investigation of olive stones pyrolysis via coupled thermogravimetric analysis-mass spectrometry: Thermal behavior and kinetic parameters. *Cellul. Chem. Technol.* **56**, 481–494. <https://doi.org/10.35812/CelluloseChemTechnol.2022.56.41> (2022).
8. Yu, X. et al. Co-hydrothermal conversion of kitchen waste and agricultural solid waste biomass components by simple mixture: study based on bio-oil yield and composition. *J. Anal. Appl. Pyrol.* **180**, 106557. <https://doi.org/10.1016/j.jaap.2024.106557> (2024).
9. Dai, A. et al. Walnut shell oil-bath torrefaction coupled with fast pyrolysis: Effect of torrefaction heating modes. *Bioresour. Technol.* **406**, 130984. <https://doi.org/10.1016/j.biortech.2024.130984> (2024).
10. Silva, W. R., Santos, R. M. & Wisniewski, A. Continuous rotary kiln pyrolysis of cassava plant shoot system and wide speciation of oxygenated and nitrogen-containing compounds in bio-oil by HESI and APPI-Orbitrap MS. *Bioresour. Technol.* **404**, 130915. <https://doi.org/10.1016/j.biortech.2024.130915> (2024).
11. Rubinsin, N. J. et al. An overview of the enhanced biomass gasification for hydrogen production. *Int. J. Hydrog. Energy* **49**, 1139–1164. <https://doi.org/10.1016/j.ijhydene.2023.09.043> (2024).
12. Thangarasu, V., de Oliveira, M. R., Oliveira, L. A. A., Aladawi, S. & Avila, I. Combustion characteristics and gasification kinetics of Brazilian municipal solid waste subjected to different atmospheres by thermogravimetric analysis. *Bioresour. Technol.* **403**, 130906. <https://doi.org/10.1016/j.biortech.2024.130906> (2024).
13. Jahurul, M. I., Rasul, M. G., Chowdhury, A. A. & Ashwath, N. Biofuels production through biomass pyrolysis—A technological review. *Energies* **5**, 4952–5001. <https://doi.org/10.3390/en5124952> (2012).
14. Quitain, A. T., Mission, E. G., Agutaya, J. K. C. N., Sasaki, M. & Kida, T. Chapter 11 Thermal, hydrothermal liquefaction, and electromagnetic processes for biomass conversion. In *A-Z of Biorefinery* (eds Thongchul, N. et al.) 421–446 (Elsevier, 2022).
15. Wild, M. & Calderón, C. Torrefied biomass and where is the sector currently standing in terms of research, technology development, and implementation. *Front. Energy Res.* **9**, 678492. <https://doi.org/10.3389/fenrg.2021.678492> (2021).
16. Basu, P. Chapter: Torrefaction. In *Biomass Gasification, Pyrolysis and torrefaction—Practical Design and Theory* 3rd edn (ed. Basu, P.) 93–154 (Academic Press, 2018).
17. Wang, J., Minami, E., Asmadi, M. & Kawamoto, H. Thermal degradation of hemicellulose and cellulose in ball-milled cedar and beech wood. *J. Wood Sci.* **67**, 32. <https://doi.org/10.1186/s10086-021-01962-y> (2021).
18. Butnaru, E. & Brebu, M. The thermochemical conversion of forestry residues from silver fir (*Abies alba* Mill.) by torrefaction and pyrolysis. *Energies* **15**, 3483. <https://doi.org/10.3390/en15103483> (2022).
19. Zadeh, Z. E., Abdulkhani, A., Aboelazayem, O. & Saha, B. Recent insights into lignocellulosic biomass pyrolysis: A critical review on pretreatment, characterization, and products upgrading. *Processes* **8**, 799. <https://doi.org/10.3390/pr8070799> (2020).
20. Öneç, S., Brebu, M., Vasile, C. & Yanik, J. Copyrolysis of scrap tires with oily wastes. *J. Anal. Appl. Pyrol.* **94**, 184–189. <https://doi.org/10.1016/j.jaap.2011.12.006> (2012).
21. Brebu, M., Tamminen, T. & Spiridon, I. Thermal degradation of various lignins by TG-MS/FTIR and Py-GC-MS. *J. Anal. Appl. Pyrol.* **104**, 531–539. <https://doi.org/10.1016/j.jaap.2013.05.027> (2013).
22. Vuppalladadiyam, A. K. et al. Biomass pyrolysis: A review on recent advancements and green hydrogen production. *Bioresour. Technol.* **364**, 128087. <https://doi.org/10.1016/j.biortech.2022.128087> (2022).
23. Bridgewater, A. V. Review of fast pyrolysis of biomass and product upgrading. *Biomass Bioenerg.* **38**, 68–94. <https://doi.org/10.1016/j.biombioe.2011.01.048> (2012).
24. Su, G. & Jiang, P. Machine learning models for predicting biochar properties from lignocellulosic biomass torrefaction. *Bioresour. Technol.* **399**, 130519. <https://doi.org/10.1016/j.biortech.2024.130519> (2024).
25. Wang, M., Xie, Y., Gao, Y., Huang, X. & Chen, W. Machine learning prediction of higher heating value of biochar based on biomass characteristics and pyrolysis conditions. *Bioresour. Technol.* **395**, 130364. <https://doi.org/10.1016/j.biortech.2024.130364> (2024).
26. Butnaru, E., Stoleru, E. & Brebu, M. Valorization of forestry residues by thermal methods. The effect of temperature on gradual degradation of structural components in bark from silver fir (*Abies alba* Mill.). *Ind. Crops. Prod.* **187**, 115376. <https://doi.org/10.1016/j.indcrop.2022.115376> (2022).
27. Brebu, M., Butnaru, E., Stoleru, E., Sim, S.F., Source discrimination by new approaches on classical characterization methods – a prerequisite for thermochemical conversion of agriculture. *Energy*. submitted (2025).
28. Castello, G. Retention index systems: alternatives to the n-alkanes as calibration standards. *J. Chromatogr. A* **842**, 51–64. [https://doi.org/10.1016/S0021-9673\(98\)00989-3](https://doi.org/10.1016/S0021-9673(98)00989-3) (1999).
29. Bizzo, H. R., Brilhante, N. S., Nolvachai, Y. & Marriott, P. J. Use and abuse of retention indices in gas chromatography. *J. Chromatogr. A* **1708**, 464376. <https://doi.org/10.1016/j.chroma.2023.464376> (2023).
30. Bajer, T. et al. Chemical profiling of volatile compounds of various home-made fruit spirits using headspace solid-phase microextraction. *J. Inst. Brew.* **123**, 105–112. <https://doi.org/10.1002/jib.386> (2017).
31. Debevc, S. et al. Valorization of almond shell biomass to biocarbon materials: Influence of pyrolysis temperature on their physicochemical properties and electrical conductivity. *Carbon Trends* **9**, 100214. <https://doi.org/10.1016/j.cartre.2022.100214> (2022).
32. Vasile, C., Popescu, C. M., Popescu, M. C., Brebu, M. & Willfor, S. Thermal behaviour/treatment of some vegetable residues. IV. Thermal decomposition of eucalyptus wood. *Cellul. Chem. Technol.* **45**, 29–42 (2011).
33. Febrero, L., Granada, E., Pérez, C., Patiño, D. & Arce, E. Characterisation and comparison of biomass ashes with different thermal histories using TG-DSC. *J. Therm. Anal. Calorim.* **118**, 669–680. <https://doi.org/10.1007/s10973-014-3717-3> (2014).
34. Souza, A. G., Oliveira Santos, J. C., Conceição, M. M., Dantas Silva, M. C. & Prasad, S. A thermoanalytic and kinetic study of sunflower oil. *Braz. J. Chem. Eng.* **21**, 265–273. <https://doi.org/10.1590/S0104-66322004000200017> (2004).
35. Santos, J. C. O., Dos Santos, I. M. G., De Souza, A. G., Prasad, S. & dos Santos, A. V. Thermal stability and kinetic study on thermal decomposition of commercial edible oils by thermogravimetry. *J. Food Sci.* **67**, 1393–1398. <https://doi.org/10.1111/j.1365-2621.2002.tb10296.x> (2002).
36. Murata, K. & Makino, T. Thermal degradation of polypropylene. *Nippon Kagaku Kaishi* <https://doi.org/10.1246/nikkashi.1975.192> (1975).
37. Zhou, S., Xue, Y., Sharma, A. & Bai, X. Valorization through thermochemical conversion: comparison of hardwood, softwood and herbaceous lignin. *ACS Sustain. Chem. Eng.* **4**, 6608–6617. <https://doi.org/10.1021/acssuschemeng.6b01488> (2016).
38. Brebu, M., Bhaskar, T., Muto, A. & Sakata, Y. Alkaline hydrothermal treatment of brominated high impact polystyrene (HIPS-Br) for bromine and bromine-free plastic recovery. *Chemosphere* **64**, 1021–1025. <https://doi.org/10.1016/j.chemosphere.2006.02.036> (2006).
39. Chemeo a. <https://www.chemeo.com/cid/34-071-5/m-Guaiacol>. Accessed 30 Sep 2024. (2024).
40. Chemeo b. <https://www.chemeo.com/cid/18-688-9/Phenol-2-6-dimethoxy>. Accessed 30 Sep 2024. (2024).
41. Vasile, C. & Brebu, M. A. Thermal valorisation of biomass and of synthetic polymer waste. Upgrading of pyrolysis oils. *Cell. Chem. Technol.* **40**, 489–512 (2006).
42. Stoleru, E. & Brebu, M. Stabilization techniques of essential oils by incorporation into biodegradable polymeric materials for food packaging. *Molecules* **26**, 6307. <https://doi.org/10.3390/molecules26206307> (2021).
43. Zhang, L. et al. Research of the two-step pyrolysis of lignocellulosic biomass based on the cross-coupling of components by Py-GC/MS. *Biomass Conv. Biorefin.* **13**, 11789–11802. <https://doi.org/10.1007/s13399-021-01993-x> (2021).

44. Mettler, M. S. et al. Revealing pyrolysis chemistry for biofuels production: Conversion of cellulose to furans and small oxygenates. *Energy Environ. Sci.* 5, 5414–5424. <https://doi.org/10.1039/C1EE02743C> (2012).

Acknowledgements

This work was supported by the grant from the Ministry of Research, Innovation and Digitization, CNCS/CCCDI-UEFISCDI, Romania, project code PN-III-P4-PCE-2021-1141, contract number PCE 65/2022, within PNCDI III. Support from Dr. Sim Siong Fong for developing Matlab packages for Fisher weigh analysis and from Dr. Elena Butnaru and Dr. Daniela Pamfil for help with calorific value measurements is gratefully acknowledged.

Author contributions

M. B.: conceptualization, investigation, methodology, software, writing—original draft, review & editing; D. I.: investigation; E.S.: methodology, writing – original draft, review.

Declarations

Competing interests

The authors declare no competing interests.

Additional information

Supplementary Information The online version contains supplementary material available at <https://doi.org/10.1038/s41598-025-88001-8>.

Correspondence and requests for materials should be addressed to M.B.

Reprints and permissions information is available at www.nature.com/reprints.

Publisher's note Springer Nature remains neutral with regard to jurisdictional claims in published maps and institutional affiliations.

Open Access This article is licensed under a Creative Commons Attribution-NonCommercial-NoDerivatives 4.0 International License, which permits any non-commercial use, sharing, distribution and reproduction in any medium or format, as long as you give appropriate credit to the original author(s) and the source, provide a link to the Creative Commons licence, and indicate if you modified the licensed material. You do not have permission under this licence to share adapted material derived from this article or parts of it. The images or other third party material in this article are included in the article's Creative Commons licence, unless indicated otherwise in a credit line to the material. If material is not included in the article's Creative Commons licence and your intended use is not permitted by statutory regulation or exceeds the permitted use, you will need to obtain permission directly from the copyright holder. To view a copy of this licence, visit <http://creativecommons.org/licenses/by-nc-nd/4.0/>.

© The Author(s) 2025